Received: 11 March 2019 | Revised: 23 August 2019 | Accepted: 4 September 2019

DOI: 10.1002/jhet.3751

WILEY

ARTICLE

An expeditious synthesis of 2,3-dihydroquinozoline-4(1*H*)-ones using graphene-supported sulfonic acid

Shivanand Gajare | Megha Jagadale | Altafhusen Naikwade | Prakash Bansode | Pradnya Patil | Gajanan Rashinkar

Department of Chemistry, Shivaji University, Kolhapur, India

Correspondence
Gajanan Rashinkar, Department of Chemistry, Shivaji University, Kolhapur, 416004, Maharastra, India.
Email: gsr_chem@unishivaji.ac.in

Abstract

Graphene-supported sulfonic acid ($Gr@SO_3H$) has been prepared by covalent grafting of (3-mercaptopropyl)trimethoxysilane in the matrix of graphene followed by treatment with sulfuric acid and hydrogen peroxide. $Gr@SO_3H$ has been successfully characterized by Fourier transform infrared (FT-IR) spectroscopy, Fourier transform Raman (FT-Raman) spectroscopy, CP-MAS ^{13}C NMR spectroscopy, thermogravimetric analysis (TGA), energy dispersive X-ray analysis (EDX), transmission electron microscopy (TEM), Brunauer-Emmett-Teller (BET) analysis, and X-ray diffractometer (XRD) analysis. $Gr@SO_3H$ served as a robust heterogeneous catalyst for the synthesis of bioactive 2,3-dihydroquinazolin-4(1*H*)-ones from anthranilamide and aryl aldehydes in ethanol. Recyclability experiments were executed successfully for six consecutive runs.

1 | INTRODUCTION

The recent quest to develop environmentally benign processes has spurred extensive interest in the use of heterogeneous Bronsted acids in organic synthesis.[1] The use of heterogeneous Bronsted acids provide the ultimate benefit of low waste and circumvent the environmental and personal toxicity concerns associated with the homogeneous Bronsted acid.[2] In addition, their immiscibility with common organic solvents, excellent catalytic performance, high air, thermal and chemical stability, non-hygroscopic nature, easy separation from reaction media, and facile recyclability make their utilization economically feasible.[3] Owing to these distinct features, they find myriad of applications in the production of fine chemicals, pharmaceuticals, polymers, biodiesel as well as in oil refining and petroleum industries.[4] The scrutiny of literature reveals that the performance of heterogeneous Bronsted acids primarily depends on the nature of support.[5] In view of this, a large number of distinct supports such as activated carbon, periodic mesoporous organosilica, polypropylene fiber, polyethylene glycol, metal oxides, and zeolites[6] have been employed in the preparation of heterogeneous Bronsted acids.

Nanomaterials play a crucial role in green chemistry as they improve the environmental sustainability of processes producing negative externalities. They display striking features such as small size, extensive surface to volume proportion and ease of surface functionalization. Recently, graphene oxide (GO) has emerged as a promising nanomaterial that has been conventionally related in wide areas. The applications of GO offers real points of interest inferable from its remarkable physical, electronic, and chemical properties such as electroconductivity, amphiphilicity, fluorescence quenching capacity, surface-enhanced Raman scattering (SERS) property, and amazing aqueous processability.[7] Owing to these properties, GO has attracted tremendous attention in drug delivery, organic synthesis, diagnostics, cancer therapy, tissue engineering, electrochemistry, and imaging sensors.[8] GO and its composites are used as reusable adsorbents for removal/enrichment of

inorganic/organic substances in aqueous solutions, rare earth elements, and hazardous materials for environmental safety and human health.[9] In the recent years, GO has emerged as unparalleled 2D support in the preparation of heterogeneous catalysts due to large surface area, high loading of active sites, amphiphilic nature, excellent dispersibility, and resistance to degradation in both acidic and basic media. In addition, GO can be easily decorated with active functional groups such as amines, acids, thiols, and thioethers.[10] Among various GO-based heterogeneous catalysts, graphene supported sulfonic acid has attracted considerable attention as a heterogeneous Bronsted acid for a variety of acid-catalyzed reactions.[11]

Heterocycles constitute one of the most privileged compounds endowed with high structural complexity and diversity. 2,3-Dihydroquinazolin-4(1*H*)-ones represent one of the most important class of heterocycles that possess meritorious biological activities including anticancer, anticonvulsant, antihypertensive, diuretic, antibacterial, and monoamine oxidase inhibition[12] properties. In addition, they are commonly encountered scaffolds in commercial drugs such as Afloqualone (sedative, hypnotic, anticancer, anti-anxiety agents), Etaqualone (nervous system depressant), and Rutaecarpine (Alzheimer's disease).[13] In view of their significant properties, a variety of distinct protocols have been developed for the synthesis of 2,3-dihydroquinazolin-4(1*H*)-ones.[14] Among various methods, cyclization of anthranilamide with aryl aldehyde represents one of the most prominent and elegant method for synthesis of 2,3-dihydroquinazolin-4(1*H*)-ones. A large number of catalysts including nano-MgO, Sc(III)-inda-pybox, cerium (III) chloride, $TiCl_4$/Zn, β-cyclodextrin, $SnCl_2.H_2O$, ceric (IV) ammonium nitrate (CAN), amberlyst-15, ionic liquids, tetrabutyl ammonium bromide, Bronsted acid, and phosphoric acid[15] have been employed to increase the efficiency of this protocol. However, despite impressive progress, a thrust toward developing environmentally benign procedure using highly efficient heterogeneous catalyst is a subject of immense research in organic synthesis.

In continuation of our research toward applications of nanomaterials in catalysis,[16] we report herein an expeditious synthesis of 2,3-dihydroquinozoline-4(1*H*)-ones by cyclization of anthranilamide with aryl aldehyde using graphene-supported sulfonic acid.

2 | RESULTS AND DISCUSSION

The preparation of graphene-supported sulfonic acid is outlined in Scheme 1. Initially, purified graphite (**1**) was oxidized to graphite oxide (**2**) following modified Hummers and Offeman method.[17,18] The ultrasound-assisted exfoliation of **2** using hydrazine hydrate in aqueous medium afforded GO (**3**) which was subsequently treated with (3-mercaptopropyl)trimethoxysilane to form mercaptopropyl graphene (**4**). Finally, the oxidation of thiol

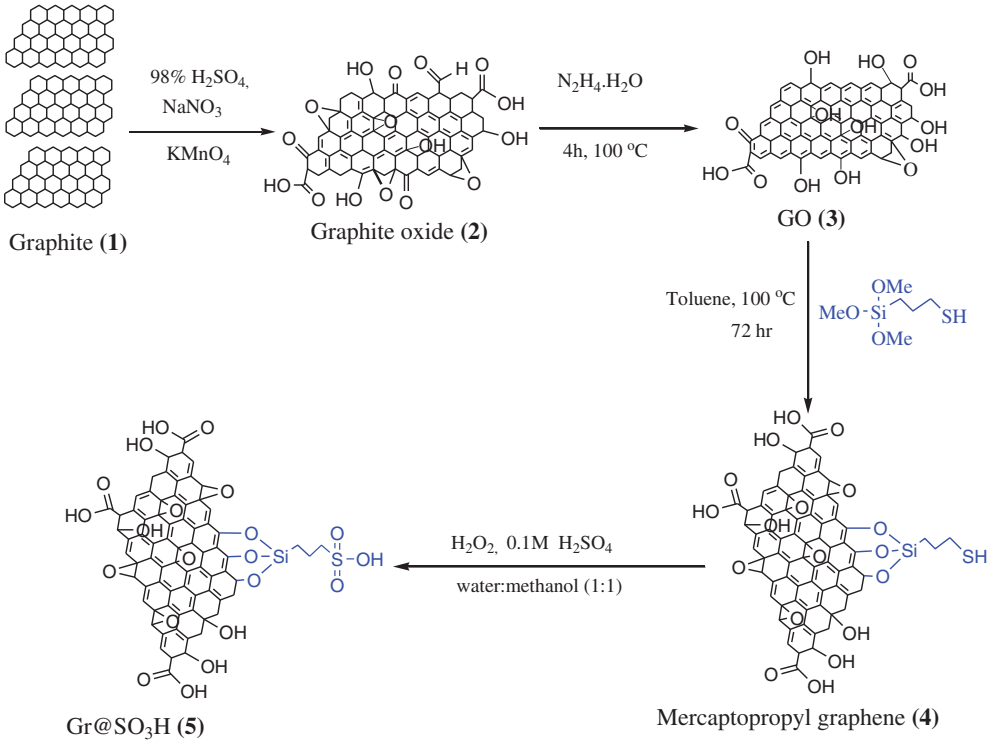

SCHEME 1 Preparation of Gr@SO_3H (**5**)

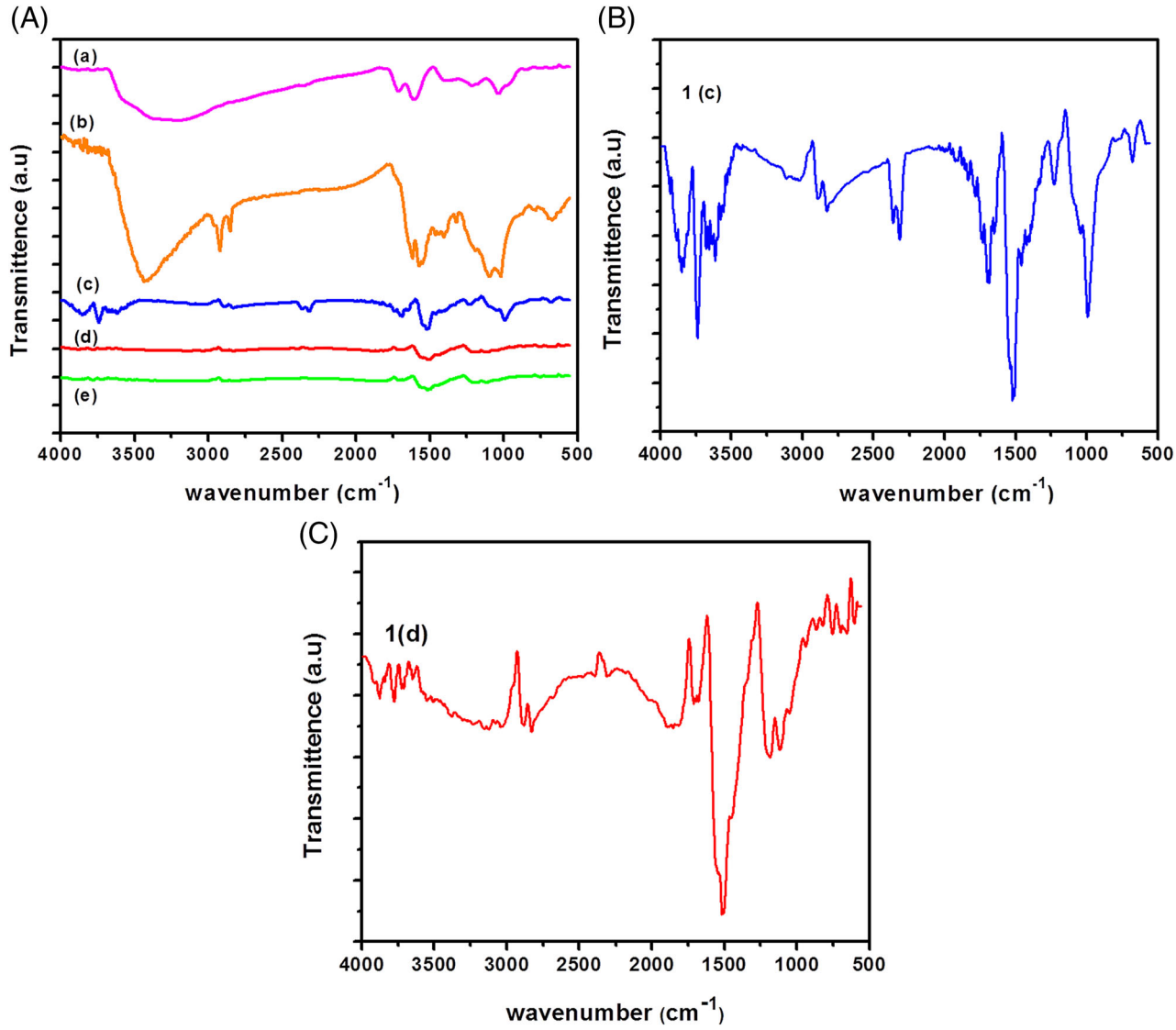

FIGURE 1 FT-IR spectra of (a) graphite oxide (**2**); (b) GO (**3**); (c) mercaptopropyl graphene (**4**); (d) Gr@SO_3H (**5**); (e) reused Gr@SO_3H (**5**); (B) mercaptopropyl graphene (4); (C) Gr@SO_3H (5)

groups in **4** with sulfuric acid and hydrogen peroxide afforded desired graphene-supported sulfonic acid acronymed as Gr@SO_3H (**5**). Fourier-transform infrared (FT-IR) and FT-Raman spectroscopy were used to monitor reactions involved in the preparation of Gr@SO_3H (**5**). The FT-IR spectrum (Figure 1a) of graphite oxide (**2**) displayed *characteristic* peaks at 1611 cm^{-1} (C═C stretching), 1388 cm^{-1} (C—O stretching) and 1037 cm^{-1} (C—O stretching). The formation of GO (**3**) was reflected by typical absorptions at 1718 cm^{-1} (C═O stretching) and 3435 cm^{-1} (O—H stretching) in the FT-IR spectrum (Figure 1b). Successful grafting of mercaptopropyl group in **4** was confirmed by FT-IR spectrum (Figure 1c) on the basis of peaks at 2892 cm^{-1} (C—H stretching), 2362 cm^{-1} (S—H stretching), and 1116 cm^{-1} (Si—O stretching).[19] In the FT-IR spectrum of **5**, characteristic peaks at 1186 cm^{-1} (asymmetric stretching of S═O of sulfonate group) and 1053 cm^{-1} (symmetric stretching of S═O of sulfonate group) confirmed the presence of SO_3H demonstrating the successful formation of Gr@SO_3H (**5**) (Figure 1d).[20]

The surface modification of GO was also reflected in the FT-Raman spectroscopy. Raman spectra of GO (**3**) **(**-Figure 2A**)** and Gr@SO_3H **(5) (**Figure 2B) displayed characteristic D, G, 2D, and D + G bands. The D band is attributed to vibrations of sp^3 carbon atoms related to defected and disordered lattices, whereas the G band arises from the vibration of sp^2 carbon atoms in graphene lattices.[21,22] The 2D peak is associated with second order-disorder mode from a different in-plane vibration

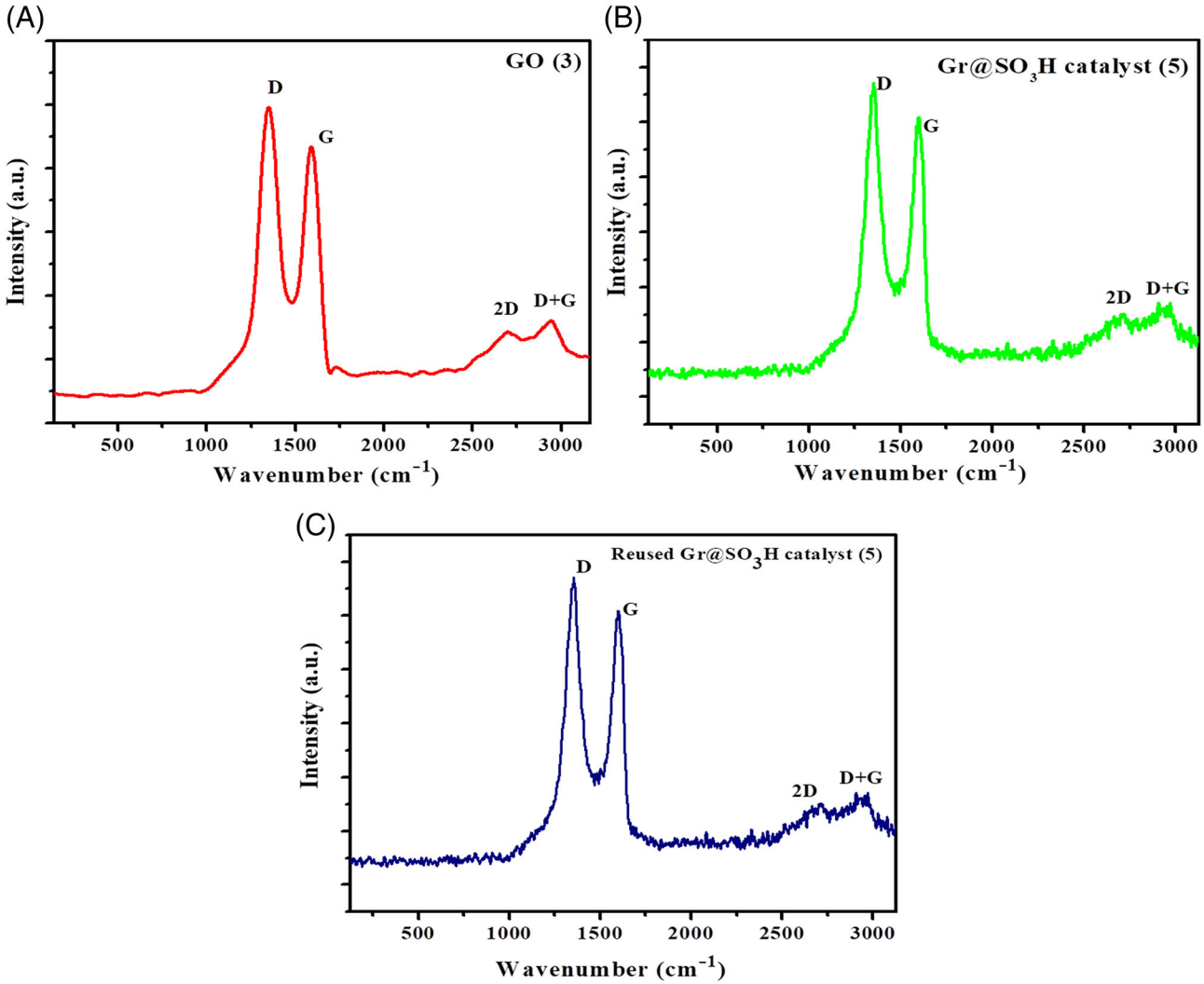

FIGURE 2 (A) Raman spectrum of GO (3) (red), (B) Raman spectrum of Gr@SO_3H (**5**) (green), and (C) Raman spectrum of reused Gr@SO_3H (**5**) (blue)

and D + G is combination scattering peak. The D and G band peaks in **3** were observed at 1358 and 1600 cm^{-1}, respectively. The D and G band peaks for **5** became narrower in shape and were displayed at 1351 and 1588 cm^{-1} indicating slight redshift due to reordering in the structure during reduction and sulfonation process thereby providing additional evidence for the formation of **5**.[23]

The thermal stability of Gr@SO_3H **(5)** was assessed by TGA analysis over the temperature range of 25-1000°C at heating rate of 10°C/minute (Figure 3). The initial weight loss of 6.7% up to 91°C is due to desorption of physically adsorbed water. The second key weight loss of 14.9% up to 465°C is attributed to loss of oxygen-containing groups such as CO and CO_2[24,25] as well as liberation of SO_3H group from GO surface.[26] The final weight loss of 59.7% up to 735°C is ascribed to the complete combustion of GO and carbon skeleton.[27]

Brunauer-Emmett-Teller (BET) surface area analysis was performed to evaluate the textural properties of Gr@SO_3H (**5**). The **5** showed BET surface area of 80.41 m^2/g with the average pore diameter of 35 Å. The surface area, pore-volume, and pore size of **5** was significantly increased as compared to pristine GO (77 m^2/g, 23 Å) indicating substantial grafting of SO_3H functional groups on the surface of GO.[28] The increase in surface area after hydrothermal reduction shows enhancement of porosity with increased pore size distribution which is attributed to surface modification of GO.[29,30]

The energy dispersive X-ray (EDX) analysis of Gr@SO_3H (**5**) revealed carbon and oxygen as the major elements which are attributed to GO skeleton whereas displayed minor peaks for silicon and sulfur. The presence of sulfur in its respective energy position at 2.2-2.3 keV supports the formation of **5**.[31] Furthermore, the quantification of SO_3H groups in **5** was performed by

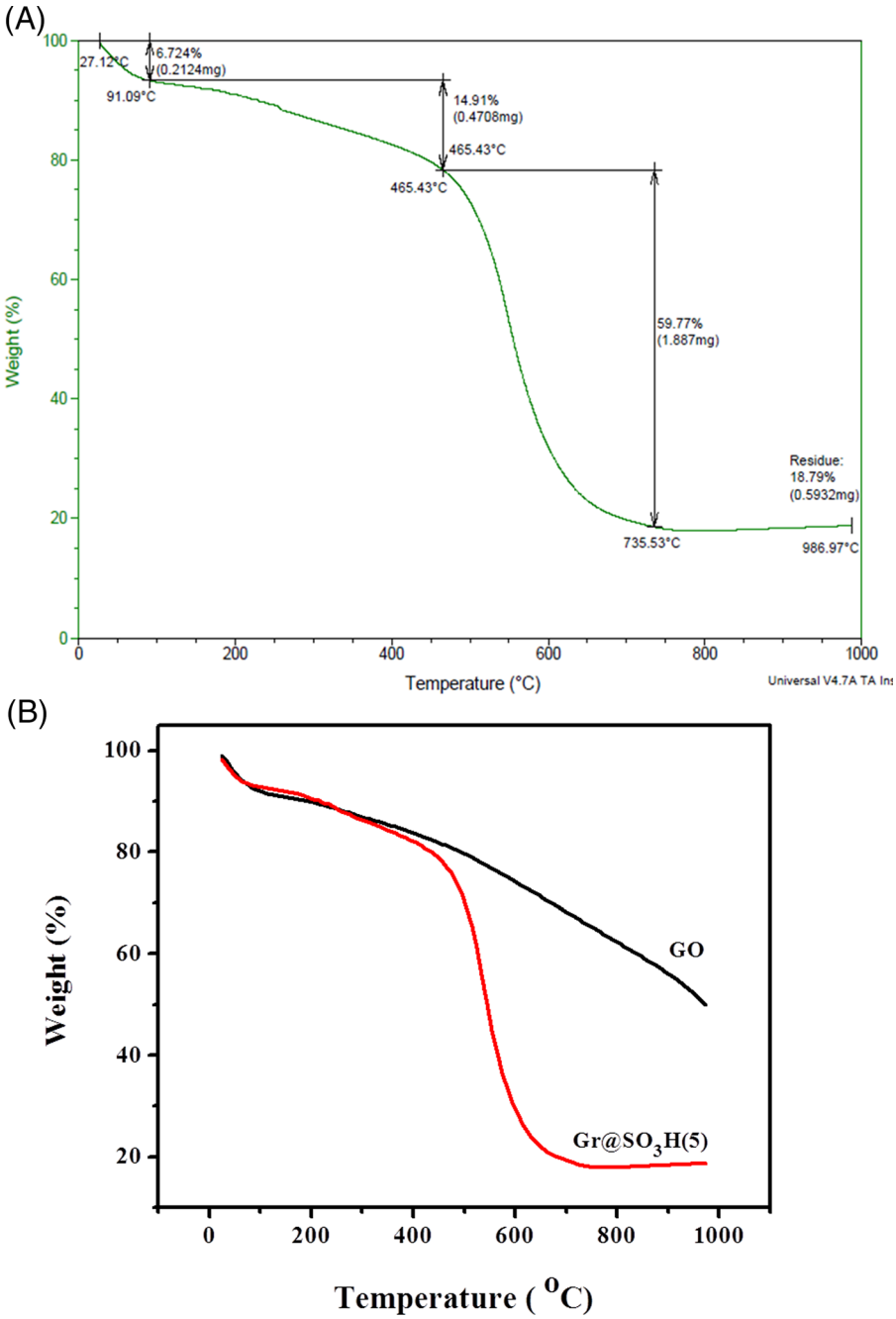

FIGURE 3 (A) TGA curve of Gr@SO_3H (**5**); (B) TGA curves of GO (**3**) and Gr@SO_3H (**5**)

volumetric titration analysis[32] and was found to be 0.14 mmol/g of **5**.

The morphology of Gr@SO_3H (**5**) was investigated by transmission electron microscopy (TEM). The TEM image of **5** and GO (**3**) (Figure 4a-c, f) displayed agglomerated, wrinkled and folded sheet-like structure which is in consistent with graphene sheet structure and crumpling features with twisted nanosheets in disordered phase.[33] The GO nanosheets carry immobilized spherical dense spots which are attributed to the presence of SO_3H groups. The selected area electron diffraction (SAED) pattern exhibits diffused ring pattern that persuades amorphous nature of GO nanosheets.[34]

The structures of pristine GO (**3**) (Figure 5A) and Gr@SO_3H (**5**) (Figure 5B) were also investigated by X-ray diffraction (XRD) analysis. The diffractograms of GO and **5** displayed two characteristic peaks at 2θ values 26.0° and 43.3° which are attributed to (002) and (101) reflections of graphitized carbon. The XRD analysis revealed retention of pristine GO in **5** even after multi-step functionalization.[35]

Our next task was to access the catalytic activity of Gr@SO_3H (**5**) for the synthesis of 2,3-dihydroquinazoline-4(1*H*)-ones. The reaction between anthranilamide **(6a)** and benzaldehyde **(7a)** was chosen as a model reaction for the optimization of reaction conditions (Scheme 2). Initially,

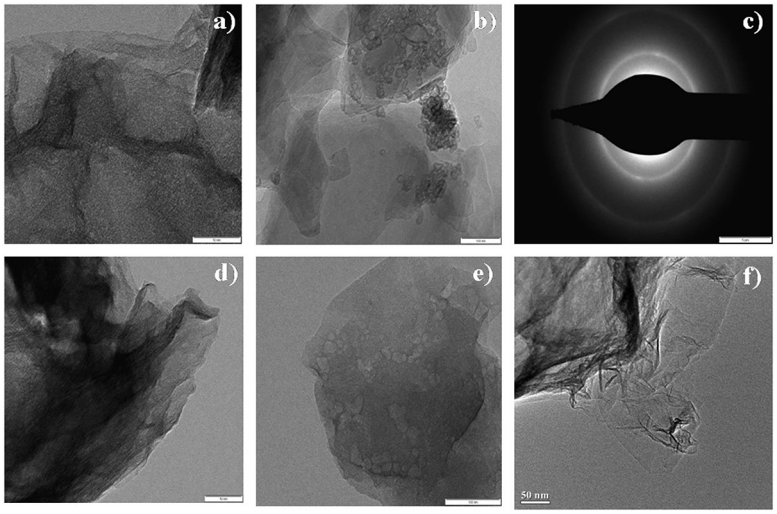

FIGURE 4 TEM images of (a-c) Gr@SO_3H (**5**) with SAED pattern; (d-e) reused Gr@SO_3H (**5**), (f) GO (**3**)

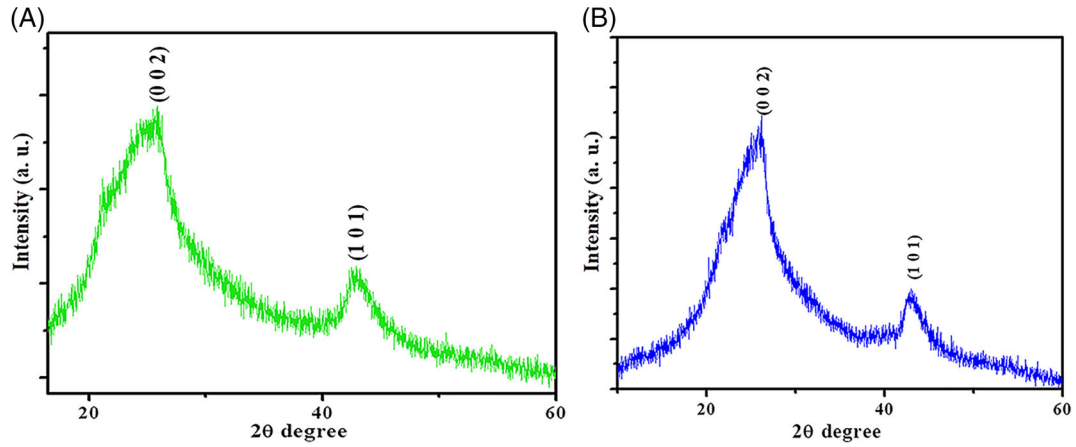

FIGURE 5 (A) XRD of GO (3) and (B) XRD of Gr@SO_3H (5)

the influence of catalyst loading on 2,3-dihydroquinazoline-4(1*H*)-one synthesis was investigated by employing various amounts of **5** (Table 1). Use of 50 mg (0.0065 mmol), 60 mg (0.0078 mmol), and 70 mg (0.0091 mmol) of **5** provided moderate yield of corresponding product *viz.* 2-phenyl-2,3-dihydroquinazoline-4-(1*H*)-one **(8a)** even after prolonged reaction time (Table 1, entries 1-3). More efficient results were obtained by using 80 mg (0.010 mmol) of **5** which boosted the yield up to 92% (Table 1, entry 4). Subsequently, further increase in the quantity of **5** did not show a substantial enhancement in the yield of product and reaction time (Table 1, entries 5-8).

The next parameter in the optimization studies was the choice of solvent. A thorough screening of different solvents was carried out (Table 2). An array of solvents including water, ethanol, toluene, acetonitrile, THF, DMF, and DCM was employed for this purpose. The model reaction afforded good yields in polar aprotic solvents such as tetrahydrofuran (THF), dimethylformamide

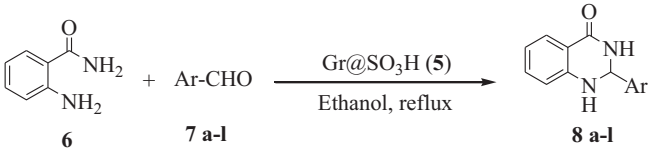

6 7 a-l 8 a-l

SCHEME 2 Synthesis of 2,3-dihydroquinazoline-4(1*H*)-ones using Gr@SO_3H (**5**)

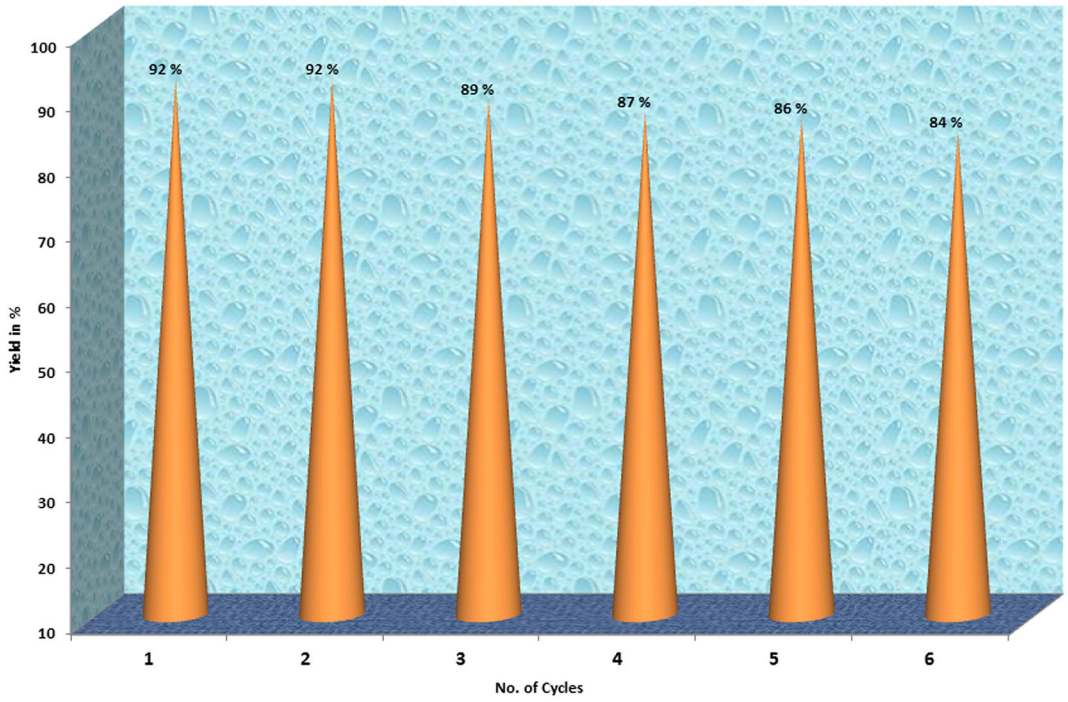

FIGURE 6 Reusability of Gr@SO_3H (**5**) in the synthesis of 2,3-dihydroquinazoline-4-(1H)-ones

TABLE 1 Optimization of catalyst loading for the synthesis of 2,3-dihydroquinazolin-4-(1*H*)-ones

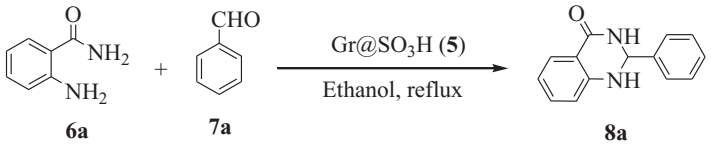

Entry	Catalyst (mg)	Time (minute)	Yield[a] (%)
1.	50	65	72
2.	60	65	78
3.	70	55	81
4	**80**	**35**	**92**
5	90	35	92
6.	100	30	92
7.	150	30	93
8.	200	30	93

Note: Reaction conditions: anthranilamide (1.0 mmol), benzaldehyde (1.0 mmol), ethanol (5 mL).
[a]Isolated yields after chromatography.

(DMF), and dichloromethane (DCM) (Table 2, entries 5-7), whereas moderate yields were obtained in nonpolar solvents like toluene (Table 2, entry 3). To our surprise, the reaction gave poor yield in water (Table 2, entry 1) and polar protic solvent such as acetonitrile (Table 2, entry 4). Among all the screened solvents, ethanol gave excellent yield of the desired product and hence it was selected for further studies (Table 2, entry 2).

After procuring the optimized reaction conditions, we probed the general applicability of protocol by reacting anthranilamide **(6a)** with a variety of substituted aryl aldehydes **(7a-l)**. The results are summarized in Table 3. The results indicate that both electron-rich as well as electron-deficient aryl aldehydes reacted efficiently with anthranilamide giving excellent yields of corresponding products (Table 3, entry **8a-l**). It is worth mentioning that

TABLE 2 Optimization of solvent in synthesis of 2,3-dihydroquinazoline-4(1*H*)-ones

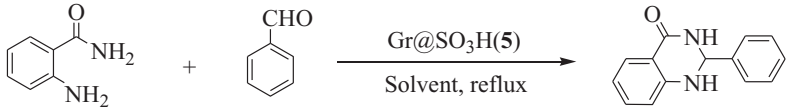

6a **7a** **8a**

Entry	Solvent	Time (minute)	Yield[a] (%)
1	Water	240	40
2	**Ethanol**	**35**	**92**
3	Toluene	55	82
4	Acetonitrile	130	60
5	THF	55	88
6	DMF	360	90
7	DCM	65	78

Note: Reaction conditions: anthranilamide (1.0 mmol), benzaldehyde (1.0 mmol), solvent (5 mL).
[a]Isolated yields after chromatography.

heterocyclic aromatic aldehydes such as thiophene-2-carbaldehyde (Table 3, entry **7j**), furan-2-carbaldehyde (Table 3, entry **7k**) and pyridine-4-aldehyde (Table 3, entry **7l**) afforded corresponding products in high yields (Table 3, entries **8j-l**, 90-92%). As expected, *o*-chloro benzaldehyde afforded lower yield of desired quinozoline due to steric hindrance (Table 3, entry **8e**).

The plausible mechanism for Gr@SO_3H (**5**) promoted the synthesis of 2,3-dihydroquinazolin-4(1*H*)-ones postulated on the basis of literature reports and is depicted in Scheme 3.[36,37] Initially, **5** activate carbonyl group of aldehyde (**I**) *via* co-ordination with carbonyl oxygen. This facilitates the reaction of aryl aldehydes with anthranilamide (**II**) generating imine intermediate (**III**). Furthermore, **5** activates imine group of **III** thus accelerating intramolecular nucleophilic attack of carboximidate nitrogen on imine carbon affording the desired product (**IV**).

In order to confirm the heterogeneous nature of the Gr@SO_3H (**5**), a hot filtration test was implemented employing the model reaction. The catalyst was filtered off when a 50% conversion was accomplished (GC). The filtrate of reaction mixture was stirred for additional 3 hours. Interestingly, there was no enhancement in the yield of product beyond 50% confirming the heterogeneous nature of **5**.

Reusability is one of the significant features of heterogeneous catalysts for more efficient and economical processed. The recyclability of Gr@SO_3H (**5**) was scrutinized by repeating the model reaction (Figure 6). In brief, once the reaction was completed, the reaction mixture was centrifuged and the recovered **5** was washed several times with ethanol, dried in vacuum at room temperature and used for recyclability studies. The **5** showed unprivileged recycling performance as there was a significant decrease in the product yield with the prolonged reaction time during each successive run. The decline in catalytic potential was elucidated based on inflation of reactant and product molecules that might be hooked up the catalyst sites. Therefore, we attempted reusability studies after reactivation at each cycle. The reactivation involved vacuum treatment of **5** after separation and washing with ethanol, so as to remove captivated reactant and product moieties on the surface. The reactivation resulted in improved catalytic performance. The quantities of reactants were calculated based on recovered catalyst. The studies revealed that **5** could be reused for six successive runs without significant diminution of catalytic activity.

The stability of recycled Gr@SO_3H (**5**) was investigated by FT-Raman spectroscopy, FT-IR spectroscopy, EDX, and TEM analysis of fresh as well as recycled Gr@SO_3H (**5**). It is noteworthy to mention that, the FT-IR (Figure 1e) and FT-Raman (Figure 2C) spectra of reused **5** still retains the prominent peak pattern of the fresh **5**, indicating that the structure of **5** remains intact during the course of the reaction. The EDX mapping of **5** after six catalytic cycles clearly confirmed the integrity of the recycled catalyst. Moreover, TEM analysis of fresh (Figure 4a-c) and reused **5** (Figure 4d,e) designates that morphology is preserved even after six successive runs. These results confirmed that the structural rigidity and main characteristics of Gr@SO_3H (**5**) remain conserved,

TABLE 3 Gr@SO_3H (5) catalyzed the synthesis of 2,3-dihydroquinazolin-4(1*H*)-ones

Entry	Anthranilamide (6)	Aldehyde (7)	Product (8)	Time (minute)	Yield (%)

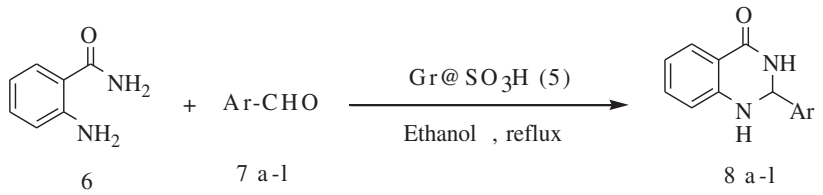

6 7 a-l 8 a-l

Entry	Anthranilamide (6)	Aldehyde (7)	Product (8)	Time (minute)	Yield[b] (%)
a	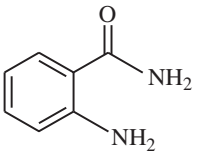	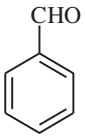	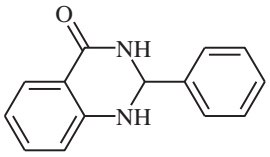	35	92
b	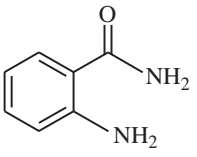	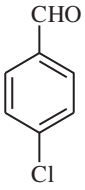	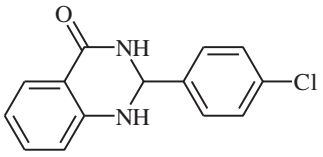	40	92
c	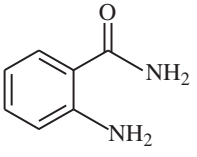	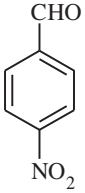	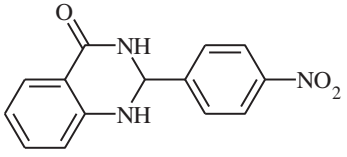	40	90
d	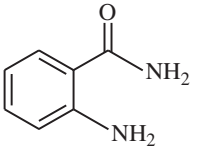	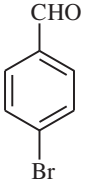	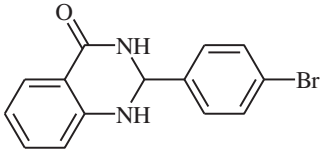	40	78
e	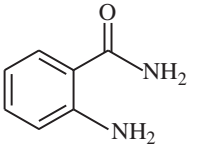	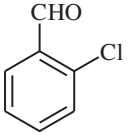	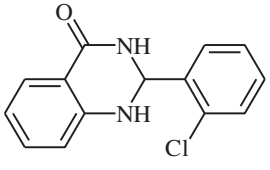	35	80
f	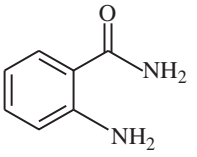	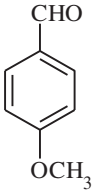	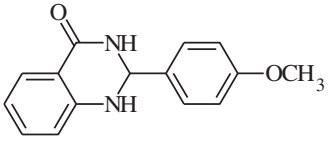	45	90

(Continues)

TABLE 3 (Continued)

Entry	Anthranilamide (6)	Aldehyde (7)	Product (8)	Time (minute)	Yield (%)
g	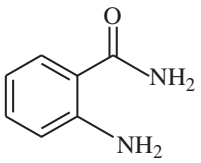	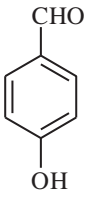	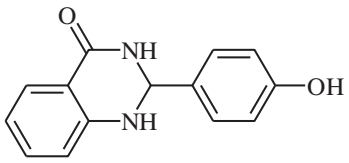	50	88
h	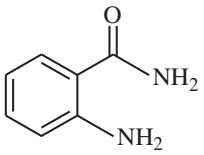	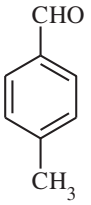	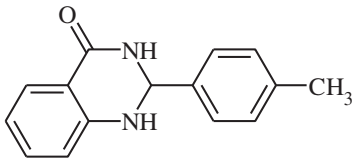	40	92
i	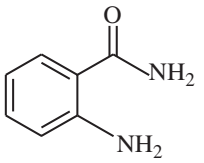	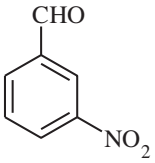	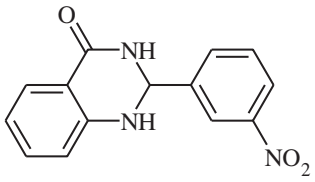	35	90
j	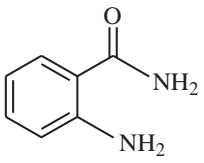	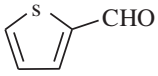	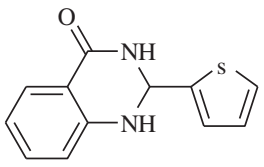	32	92
k	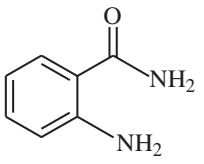	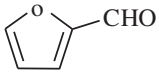	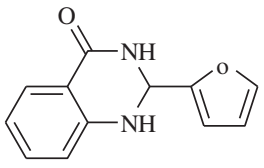	35	90
l	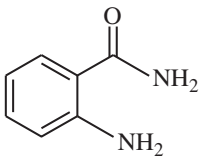	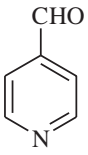	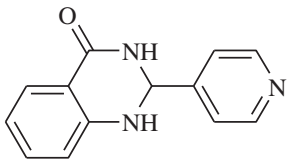	35	91

[a]Reaction conditions: anthranilamide (1. mmol), aldehydes (1.0 mmol), ethanol (5mL), Gr@SO3H (5) catalyst (80mg).
[b]Isolated yields after chromatography.

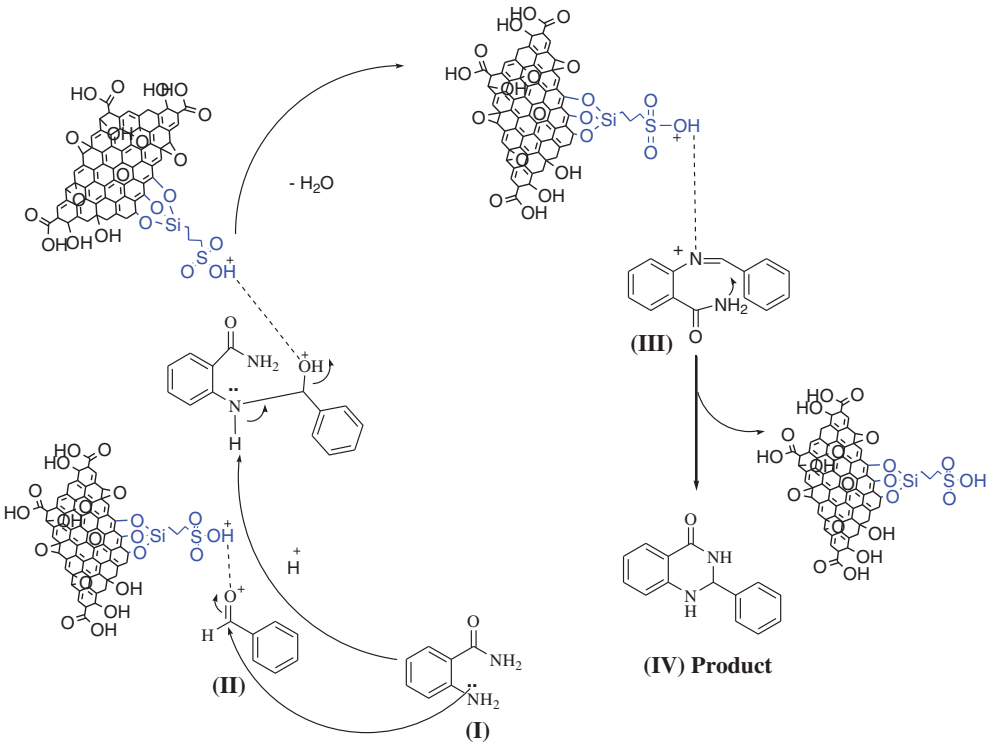

SCHEME 3 Plausible mechanism for the synthesis of 2,3-dihydroquinazolin-4(1*H*)-ones using gr@SO_3H (**5**)

demonstrating stability of **5** even after six consecutive runs.

3 | CONCLUSION

In conclusion, we have reported an expeditious synthesis of 2,3-dihydroquinazoline-4(1*H*)-ones from intermolecular cyclization between antranilamide and aryl aldehydes by using graphene-supported sulfonic acid Gr@SO_3H (**5**). The present protocol offers several striking advantages such as less reaction time, good yields, simple workup procedure, use of environmentally benign solvent, and shorter reaction time.

4 | EXPERIMENTAL

4.1 | General remarks

All reactions were carried out under air atmosphere in dried glassware. FT-IR spectra were measured with a PerkinElmer FT-IR spectrophotometer. The samples were examined as KBr discs (≈ 5% w/w). Raman spectroscopy was done using a Bruker: RFS 27 spectrometer. The thermal gravimetric analysis (TGA) curves were obtained using instrument TA SDT Q600 V20.9 Build 20 in the presence of static air at a linear heating rate of 10°C/minute from 25°C to 1000°C. Elemental analyses were performed in a PerkinElmer 2400. ^{1}H NMR and ^{13}C NMR spectra were recorded with a Bruker AC (300 MHz and 400 MHz for ^{1}H NMR and 75 and 100 MHz for ^{13}C NMR) spectrometer using $CDCl_3$ and DMSO-d6 as solvents and tetramethylsilane as an internal standard. Chemical shifts are expressed in parts per million (ppm) and coupling constants are expressed in hertz (Hz). The CP-MAS ^{13}C NMR spectrum was recorded with a JEOL-ECX400 type FT-NMR spectrometer under prescribed operating conditions. Mass spectra were recorded with a Shimadzu QP2010 GC-MS. The materials were analyzed by TEM using a PHILIPS CM 200 model with 20-200 kV accelerating voltages. Melting points were determined using MEL-TEMP capillary melting point apparatus and are uncorrected. Graphite (**1**) and all other chemicals were obtained from local suppliers and used without further purification.

4.2 | Preparation of graphite oxide (2)

Graphite oxide was synthesized by using modified Hummers and Offeman's method.[17,18] A mixture of **1** (5.0 g), $NaNO_3$ (2.5 g) and conc. H_2SO_4 (115 mL) was stirred *in an ice bath*. Afterward, $KMnO_4$ (15 g) was added gradually with constant stirring maintaining the temperature below 20°C. The reaction mixture was then shifted to water bath maintained temperature at 35°C and stirred for 30 minutes to produce thick paste. Afterward, distilled

water (230 mL) was added slowly, which enhances the temperature to 98°C and kept for 15 minutes. Furthermore, reaction mixture was treated with distilled water (700 mL) and 30% H_2O_2 (50 mL). The residue of graphite oxide **(2)** was washed with water until the pH 7, separated by centrifugation and dried under vacuum at 50°C. FT-IR (KBr, thin film): υ = 3400, 1711, 1611, 1388, 1215, and 1037 cm^{-1}.

4.3 | Preparation of GO (3)

A mixture of **2** (1.0 g) and distilled water (250 mL) was sonicated for 30 minutes. Subsequently, 50% hydrazine hydrate (5 mL) was added slowly. The resulting mixture was refluxed in an oil bath. After 4 hours, insoluble product was separated by centrifugation, washed with water (6 × 20 mL) and dried under vacuum at 50°C to afford GO **(3)**.

FT-IR (KBr, thin film): υ = 3435, 2920, 2851, 1718, 1096, and 1020 cm^{-1}; FT-Raman: υ = 3036, 2129, 1974, 1600, and 1358 cm^{-1}.

4.4 | Preparation of mercaptopropyl graphene (4)

A mixture of **3** (7.0 g) and (3-mercaptopropyl) trimethoxysilane (9.0 mL, 46 mmol) in toluene (50 mL) was refluxed in an oil bath. After 72 hours, the mixture was cooled and the residue was separated by centrifugation, washed with THF (3 × 5 mL) and dried under vacuum at room temperature for 10 hours to afford mercaptopropyl graphene (**4**). FT-IR (KBr, thin film): υ = 3617, 2892, 2362, 1687, 1521, 1227, and 1116 cm^{-1}.

4.5 | Preparation of Gr@SO_3H (5)

A mixture of **4** (7.0 g) was stirred in H_2O (50 mL), MeOH (50 mL), and 30% H_2O_2 (50 mL; 1:1:1) at room temperature for 24 hours. The solid was separated by centrifugation, washed with H_2O (3 × 5 mL) and dried under vacuum at 50°C. After 24 hours, the solid was treated with 0.1 N H_2SO_4 (50 mL) followed by sonication for 20 minutes. Finally, the mixture was separated by centrifugation, washed with THF (3 × 25 mL) and dried under vacuum at 50°C for 24 hours to afford Gr@SO_3H **(5)**. FT-IR (KBr, thin film): υ = 3437, 2921, 2852, 1642, 1575, 1463, 1186, and 1053 cm^{-1}. FT-Raman: υ = 3170, 2930, 2115, 1588, and 1351 cm^{-1}. Elemental analysis observed: % C 73.07, % O 24.24, % Si 2.25, and % S 0.44. ^{13}C CP-MAS NMR (500 MHz): δ 192 (C═O groups of graphene), 168 (O═C—O), 101 (O—C—O), 132 (graphitic sp^2-C), 70 (C—OH), 62 (epoxide), 8 (1**C**, —**C**H_2Si), 140 (**C**, SO_3H group).[38] Loading of SO_3H: 0.13 mmol of SO_3H g^{-1} of catalyst.

4.6 | General method for synthesis of 2,3-dihydroquinazoline-4(1*H*)-ones

A mixture of aryl aldehydes (1 mmol), anthranilamide (1 mmol), and Gr@SO_3H **(5)** (80 mg) in ethanol (5 mL) was stirred under reflux condition. The progress of the reaction was monitored by TLC. After completion of the reaction as monitored by the TLC, the reaction mixture was centrifuged to remove insoluble catalyst. Evaporation of solvent in vacuum followed by column chromatography over silica gel using petroleum ether-ethyl acetate (7:3, *v/v*) afforded pure products.

ACKNOWLEDGMENTS

We gratefully acknowledge the Indian Institute of Sciences (IISc), Bangalore, Sophisticated Analytical Instrumental Facility, Indian Institute of Technology, Bombay (IITB), Indian Institute of Technology, Madras (IITM) for providing spectral facilities, and Shivaji University Kolhapur for providing Golden Jubilee Research Fellowship (GJRF).

CONFLICT OF INTEREST

The authors declare no conflict of interest.

ORCID

Gajanan Rashinkar https://orcid.org/0000-0002-7200-5260

REFERENCES AND NOTES

[1] (a) K. S. Singh, *Catalysts* **2019**, *9*, 173. (b) E. Doustkhah, J. Lin, S. Rostamnia, C. Len, R. Luque, X. Luo, Y. Bando, K. C. -W. Wu, J. Kim, Y. Yamauchi, Y. Ide, *Chem A Eur J* **2019**, *25*, 1614.

[2] (a) J. H. Clark, *Acc Chem Res* **2002**, *35*, 791. (b) L. M. Gilbertson, J. B. Zimmerman, D. L. Plata, J. E. Hutchison, P. T. Anastas, *Chem Soc Rev* **2015**, *44*, 5758.

[3] (a) C. E. Volckmar, M. Bron, U. Bentrup, A. Martin, P. Claus, *J Catal* **2009**, *261*, 1. (b) J. Liu, *ACS Catal* **2017**, *7*, 34.

[4] (a) G. Busca, *Chem Rev* **2007**, *107*, 5366. (b) J. C. Védrine, *Catalysts* **2017**, *7*, 341. (c) M. G. Kulkarni, A. K. Dalai, *Ind Eng Chem Res* **2006**, *45*, 2901. d) A. F. Lee, K. Wilson, *Catal Today* **2015**, *242*, 3.

[5] (a) M. Hara, *Top Catal* **2010**, *53*, 805. (b) M. Hara, K. Nakajima, K. Kamata, *Sci Technol Adv Mater* **2015**, *16*, 1.

[6] (a) Q. Yang, Z. Zhang, B. Liang, *J Heterocycl Chem* **2015**, *52*, 310. (b) M. Nasr-Esfahani, D. Elhamifar, T. Amadeh, B. Karimi, *RSC Adv* **2015**, *5*, 13087. (c) X. -L. Shi, H. Yang,

M. Tao, W. Zhang, *RSC Adv* **2013**, *3*, 3939. (d) S. K. Pandey, A. Ahamd, O. P. Pandey, K. Nizamuddin, *J Heterocycl Chem* **2014**, *51*, 1233. (e) H. M. E. Hassaneen, T. A. Farghaly, *J Heterocycl Chem* **2015**, *52*, 1154. (f) N. Sapawe, *New J Chem* **2015**, *39*, 4526.

[7] (a) X. Huang, X. Qi, F. Boey, H. Zhang, *Chem Soc Rev* **2012**, *41*, 666. (b) R. Garg, N. K. Dutta, N. R. Choudhury, *Nanomaterials* **2014**, *4*, 267.

[8] (a) Y. Chen, C. Tan, H. Zhang, L. Wang, *Chem Soc Rev* **2015**, *44*, 2681. (b) V. Georgakilas, J. N. Tiwari, K. C. Kemp, J. A. Perman, A. B. Bourlinos, K. S. Kim, R. Zboril, *Chem Rev* **2016**, *116*, 5464. (c) Z. M. Liu, Z. Y. Guo, H. Q. Zhong, X. C. Qin, M. M. Wan, B. W. Yang, *Phys Chem Chem Phys* **2013**, *15*, 2961. (d) S. Z. Nergiz, N. Gandra, S. Tadepalli, S. Singamaneni, *ACS Appl Mater Interfaces* **2014**, *6*, 16395. (e) W. C. Lee, C. H. Lim, H. Shi, L. A. Tang, Y. Wang, C. T. Lim, K. P. Loh, *ACS Nano* **2011**, *5*, 7334. (f) S. J. Rowley-Neale, E. P. Randviir, A. S. Abo Dena, C. E. Banks, *Appl Mater Today* **2018**, *10*, 218.

[9] (a) X. -R. Zhao, X. Xu, J. Teng, N. Zhou, Z. Zhou, X. -Y. Jiang, F. -P. Jiao, J. -G. Yu, *Ecotox Environ Safe* **2019**, *176*, 11. (b) M. Gao, Z. Wang, C. Yang, J. Ning, Z. Zhou, G. Li, *Colloid Surf A* **2019**, *566*, 48. (c) X. Xu, J. Zou, X. -R. Zhao, F. -P. Jiao, J. -G. Yu, Q. Liu, J. Teng, *Colloid Surf A* **2019**, *570*, 127.

[10] X. Fan, G. Zhang, F. Zhang, *Chem Soc Rev* **2015**, *44*, 3023.

[11] (a) A. Kasprzak, M. Poplawska, *Chem Commun* **2018**, *54*, 8547. (b) A. V. Nakhate, G. D. Yadav, *Chem Select* **2018**, *3*, 4547. (c) F. Liu, J. Sun, L. Zhu, X. Meng, C. Qi, F.-S. Xiao, *J Mater Chem* **2012**, *22*, 5495. (d) L. Wang, D. Wang, S. Zhang, H. Tian, *Catal Sci Technol* **2013**, *3*, 1194.

[12] (a) R. S. Gouhar, M. M. Kamel, *J Heterocycl Chem* **2018**, *55*, 2082. (b) M. J. Kornet, T. Varia, W. Beaven, *J Heterocycl Chem* **1983**, *20*, 1553. (c) P. M. Chandrika, A. R. R. Rao, B. Narsaiah, M. B. Raju, *Int J Chem Sci* **2008**, *6*, 1119. (d) H. A. Parish Jr., R. D. Gilliom, W. P. Purcell, R. K. Browne, R. F. Spirk, H. D. White, *J Med Chem* **1982**, *25*, 98. (e) M. I. Marzouk, S. A. Shaker, T. A. Farghaly, M. A. El-Hashash, S. M. Hussein, *J Heterocycl Chem* **2017**, *54*, 3331. (f) R. C. Gupta, R. Nath, K. Shanker, K. P. Bhargava, K. Kishore, *J Indian Chem Soc* **1979**, *56*, 219.

[13] (a) K. Chen, K. Wang, A. M. Kirichian, A. F. Al Aowad, L. K. Iyer, S. J. Adelstein, A. I. Kassis, *Mol Cancer Ther* **2006**, *5*, 3001. (b) S. S. Parmar, K. Kishor, P. K. Seth, R. C. Arora, *J Med Chem* **1969**, *12*, 138. (c) M. Decker, *Eur J Med Chem* **2005**, *40*, 305.

[14] P. Devi, A. Srivastava, K. Srivastava, A. Bishnoi, *Curr Green Chem* **2017**, *4*, 25.

[15] (a) H. Kiyani, M. Tazari, F. Ghorbani, *Lett Org Chem* **2018**, *15*, 523. (b) M. Prakash, V. Kesavan, *Org Lett* **2012**, *14*, 1896. (c) X. Zhu, W. Ge, Y. Wei, *Polycyclic Aromat Compd* **2013**, *33*, 467. (d) D. Shi, L. Rong, J. Wang, Q. Zhuang, X. Wang, H. Hu, *Tetrahedron Lett* **2003**, *44*, 3199. (e) K. Ramesh, K. Karnakar, G. Satish, B. P. S. Anil Kumar, Y. V. D. Nageswar, *Tetrahedron Lett* **2012**, *53*, 6936. (f) M. Wang, Z. Song, T. Zhang, *J Heterocycl Chem* **2010**, *47*, 468. (g) M. Wang, J. J. Gao, Z. G. Song, L. Wang, *Chem Heterocycl Compd* **2011**, *47*, 851. (h) P. V. N. S. Murthy, D. Rambabu, G. Rama Krishna, C. Malla Reddy, K. R. S. Prasad, M. V. Basaveswara Rao, M. Pal, *Tetrahedron Lett* **2012**, *53*, 863. (i) J. Chen, W. Su, H. Wu, M. Liu, C. Jin, *Green Chem* **2007**, *9*, 972. (j) A. Davoodnia, S. Allameh, A. R. Fakhari, N. Tavakoli-Hoseini, *Chin Chem Lett* **2010**, *21*, 550. (k) M. Rueping, A. P. Antonchick, E. Sugiono, K. Grenader, *Angew Chem Int Ed* **2009**, *48*, 908. (l) X. Cheng, S. Vellalath, R. Goddard, B. List, *J Am Chem Soc* **2008**, *130*, 15786.

[16] (a) A. Naikwade, M. Jagadale, D. Kale, S. Gajare, G. Rashinkar, *Catal Lett* **2018**, *148*, 3178. (b) A. Naikwade, M. Jagadale, D. Kale, S. Gajare, P. Bansode, G. Rashinkar, *Appl Organomet Chem* **2019**, e5066.

[17] (a) W. S. Hummers, R. E. Offeman, *J Am Chem Soc* **1958**, *80*, 1339. (b) S. Gilje, S. Han, M. Wang, K. L. Wang, R. B. Kaner, *Nano Lett* **2007**, *7*, 3394. (c) N. I. Kovtyukhova, P. J. Ollivier, B. R. Martin, T. E. Mallouk, S. A. Chizhik, E. V. Buzaneva, A. D. Gorchinskiy, *Chem Mater* **1999**, *11*, 771.

[18] (a) H. Naeimi, Z. Ansarian, *Inorg Chim Acta* **2017**, *466*, 417. (b) C. Garkoti, J. Shabir, P. Gupta, M. Sharma, S. Mozumdar, *New J Chem* **2017**, *41*, 15545. (c) C. Y. Lee, Q. V. Le, C. Kim, S. Y. Kim, *Phys Chem Chem Phys* **2015**, *17*, 9369.

[19] B. Yu, X. Wang, W. Xing, H. Yang, X. Wang, L. Song, Y. Hu, S. Lo, *Chem Eng J* **2013**, *228*, 318.

[20] P. P. Upare, J. W. Yoon, M. Y. Kim, H. Y. Kang, D. W. Hwang, Y. K. Hwang, H. H. Kung, J. S. Chang, *Green Chem* **2013**, *15*, 2935.

[21] A. C. Ferrari, J. C. Meyer, V. Scardaci, C. Casiraghi, M. Lazzeri, F. Mauri, S. Piscanec, D. Jiang, K. S. Novoselov, S. Roth, A. K. Geim, *Phys Rev Lett* **2006**, *97*, 187401.

[22] J. Ji, G. Zhang, H. Chen, S. Wang, G. Zhang, F. Zhang, X. Fan, *Chem Sci* **2011**, *2*, 484.

[23] M. Brahmayya, S. -Y. Suen, S. A. Dai, *J Taiwan Inst Chem Eng* **2018**, *83*, 174.

[24] Ravikumar, K. Scott, *Chem Commun* **2012**, *48*, 5584.

[25] S. Stankovich, D. A. Dikin, R. D. Piner, K. A. Kohlhaas, A. Kleinhammes, Y. Jia, Y. Wu, S. T. Nguyen, R. S. Ruoff, *Carbon* **2007**, *45*, 1558.

[26] S. Ayyaru, Y. -H. Ahn, *J Membr Sci* **2017**, *525*, 210.

[27] S. N. Alam, N. Sharma, L. Kumar, *Graphene* **2017**, *6*, 1.

[28] W. I. Hayes, P. Joseph, M. Z. Mughal, P. Papakonstantinou, *J Solid State Electrochem* **2015**, *19*, 361.

[29] A. A. Farghali, M. Bahgat, W. M. A. Rouby, M. H. Khedr, *J Alloys Compd* **2013**, *555*, 193.

[30] A. K. Mishra, S. Ramaprabhu, *Desalination* **2011**, *282*, 39.

[31] V. Panwar, K. Cha, J. O. Park, S. Park, *Sens Actuat B* **2011**, *161*, 460.

[32] M. Saikia, L. Saikia, *RSC Adv* **2016**, *6*, 15846.

[33] Q. Huang, L. Zhou, X. Jiang, Y. Zhou, H. Fan, W. Lang, *ACS Appl Mater Interfaces* **2014**, *6*, 13502.

[34] J. I. Paredes, S. Villar-Rodil, P. Solı's-Fernandez, A. Mart'ınez-Alonso, J. M. D. Tascon, *Langmuir* **2009**, *25*, 5957.

[35] L. Jiao, Y. Hu, H. Ju, C. Wang, M. -R. Gao, Q. Yang, J. Zhu, S. -H. Yu, H. L. Jiang, *J Mater Chem A* **2017**, *5*, 23170.

[36] (a) N. Kausar, I. Roy, D. Chattopadhyay, A. R. Das, *RSC Adv* **2016**, *6*, 22320. (b) J. Wu, X. Du, J. Ma, Y. Zhang, Q. Shi, L. Luo, B. Song, S. Yang, D. Hu, *Green Chem* **2014**, *16*, 3210.

[37] (a) M. Rahman, I. Ling, N. Abdullah, R. Hashim, A. Hajra, *RSC Adv* **2015**, *5*, 7755. (b) T. M. Potewar, R. N. Nadaf,

T. Daniel, R. J. Lahoti, K. V. Srinivasan, *Synth Commun* **2005**, *35*, 231.

[38] S. Yongchao, T. S. Edward, *Nano Lett* **2008**, *8*, 1679.

SUPPORTING INFORMATION

Additional supporting information may be found online in the Supporting Information section at the end of this article.

How to cite this article: Gajare S, Jagadale M, Naikwade A, Bansode P, Patil P, Rashinkar G. An expeditious synthesis of 2,3-dihydroquinozoline-4(1*H*)-ones using graphene-supported sulfonic acid. *J Heterocyclic Chem*. 2019;1–14. https://doi.org/10.1002/jhet.3751